

GSM: GPU Accelerated Rare Events Sampling with Machine Learning Potentials

Haoting Zhang,¹ Jiuyang Shi,¹ Qiuhan Jia,¹ Junjie Wang,¹ and Jian Sun^{1,†}

¹National Laboratory of Solid State Microstructures, School of Physics and Collaborative Innovation Center of Advanced Microstructures, Nanjing University, Nanjing 210093, China.

ABSTRACT. Enhanced sampling has achieved considerable success in molecular dynamics (MD) simulations of rare events. Metadynamics (MetaD), owing to its excellent compatibility with MD engines, became one of the most popular enhanced sampling methods. With the boom of GPU computing and the advent of machine learning potentials (MLPs), high-accuracy, large-scale MD simulations have gradually become feasible. However, the corresponding GPU-based enhanced sampling tools have not yet been well adapted to this progress. To enable full-life-cycle GPU MetaD simulations, we propose the GPU Sampling MetaD (GSM) package. By leveraging MLPs, it is feasible to perform high-precision rare event sampling for systems comprising millions of atoms on a typical single GPU, which offers a potential solution to many size-dependent problems. By conducting sampling in several classical systems, the results sufficiently demonstrate the capability of this package to simulate diverse atomic systems, especially efficient in large scale systems.

I. INTRODUCTION

Molecular dynamics (MD) simulations play a critical role in investigating the structure, properties, and dynamic behavior of atomic systems [1,2]. Enhanced sampling methods brought the tool into study of rare events to accelerate slow modes in the dynamic behavior. In 1977, the umbrella sampling (US) method was introduced, in which a predefined bias potential is applied along a reaction coordinate to promote sampling of rare configurations, and unbiased free-energy surface (FES) are reconstructed via reweighting procedures [3,4]. On this basis, many enhanced sampling methods were subsequently proposed, such as replica exchange MD (REMD), metadynamics (MetaD), Gaussian accelerate MD (GaMD). Among these approaches, MetaD stands out for its combination of adaptive biasing along collective variables (CVs) and straightforward FES reconstruction, while maintaining high compatibility with conventional MD program.

In parallel with the advancement of enhanced sampling algorithms, the broader field of MD simulation has also undergone rapid development along two prominent directions. First, the construction of potential energy surface (PES) is progressively shifting toward data-driven paradigms, producing a new generation of high-accuracy machine-learning potentials (MLPs) [5–8]. Second, increasing attention is being devoted to the dynamic behavior of large-scale systems over extended timescales, such as microseconds protein folding simulations [9,10], device-scale atomistic modeling [11] and millions-electrons ab initio molecular dynamics (AIMD) study of urea nucleation [12].

In recent years, many studies have benefited from high accuracy of MLPs and GPU-accelerated MD simulations, successfully found a variety of large-scale dynamical phenomena, including several notable applications of MetaD simulations like liquid-solid phase transition [13–15] and interface water dynamics [16–18]. However, classical sampling packages have less support with the new paradigms of

MD, especially lacking a full-life-cycle GPU-based simulation framework, thereby constraining the speed and accessible scale of MetaD simulations. Building upon this foundation, our work integrates GPU-based enhanced sampling simulations into GPUMD, thereby establishing a fully GPU-enabled metadynamics simulation framework GPU Sampling MetaD (GSM). This design enables users to perform rapid and efficient enhanced sampling calculations while simultaneously benefiting from the high accuracy of MLPs.

To demonstrate the correctness, generality, and efficiency of our GSM package, and to provide users with a comprehensive enhanced sampling solution, we conducted simulation tests on molecular, interfacial, and large-scale periodic bulk systems. The results indicate that our program not only ensures accuracy and ease of use, but achieves more than a tenfold speedup compared with mainstream implementations. Our approach is expected to provide a solution for enhanced sampling simulations with greater computational demands and first-principle accuracy, helping researchers apply this paradigm to more challenging areas, such as long-chain protein folding, high-index surface catalytic reactions, and phase transition simulations of large crystal systems.

II. METHODS

A. Metadynamics Method

Since the introduction of enhanced sampling methods in 1977, bias-based enhanced sampling methods have continuously evolved and improved, maintaining strong momentum in the fields of molecular and atomic simulations [19]. Among these methods, MetaD has emerged as the preferred approach in numerous computational studies due to its high compatibility with molecular dynamics workflows and its ability to accelerate rare events [20,21]. Here, we simply introduce the fundamental procedures of MetaD and detail our implementation strategy.

In a dynamic system with a interaction potential U_0 , metadynamics works by periodically depositing bias potentials $V_b(s_\tau; \tau)$ at the states visited by the system, thus giving the biased interaction:

$$U_b(s_t) = U_0(s_t) + \sum_{\tau} V_b(s_\tau; \tau)$$

Where s_t denotes the states of the system at time t , which is usually referred to as the collective variable (CV), τ denotes the deposition frame in the simulation. Therefore it can progressively fill the minima of the free-energy surface and thus significantly increase the likelihood of transitions. In MetaD procedure, CVs typically assume distinct values corresponding to different local minima and has much lower rank than the full dynamic parameters, thus characterizing system states and slow transition modes near potential barriers. A bias potential is subsequently built, commonly by adding gaussians centered on the sampled CVs. The procedure mostly converges while the FES is filled flat, and thus it can be reconstructed by reweighting procedure:

$$P_{unbias}(s) = \frac{\langle \delta[s - s(R)] e^{\beta V_b(s)} \rangle_{U_b}}{\langle e^{\beta V_b(s)} \rangle_{U_b}}$$

$$F(s) = -\frac{1}{\beta} \log P_{unbias}(s)$$

where $\langle \cdot \rangle_{U_b}$ stands for averaging over the biased ensemble.

B. Frameworks of GPU Sampling MetaD

We will briefly introduce the workflow of GPU Sampling MetaD, including the frontend processes users interact with when using this software package, and the backend processes we have implemented for fully GPU-based simulations, which is shown in Fig. 2.

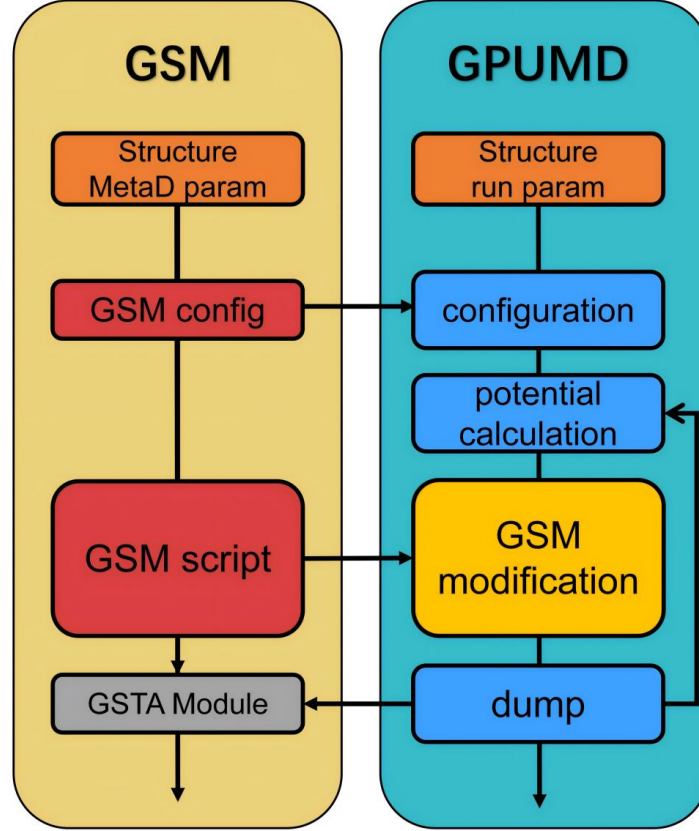


FIG 1. The flow chart of GSM and its collaboration mode with GPUMD. Users can define GSM script with a python script with configurations one wants. With our GSM-interface compiled in GPUMD, GSM script can be loaded into GPUMD workflow and automatically modify it into a MetaD workflow. Simultaneously, the GSM script can instantly turns into an analysis tool for any output MD trajectory, independent with GPUMD workflow.

In collaboration with GPUMD, we have achieved a comprehensive workflow for enhanced sampling simulations entirely implemented on GPU. GSM is developed based on PyTorch, a widely-used GPU computing framework with an extensive user base and open-source accessibility. This allows users to benefit from the ease of use and comprehensive tutorial support inherent to open-source society.

A typical enhanced sampling workflow is defined as shown in Fig.S1. Users can employ our predefined workflow templates, reference our predefined CVs, and freely combine statistical quantities using Python scripts. Additionally, users can customize CVs and biases by subclassing `torch.nn.Module`. We refer to a defined enhanced sampling workflow as a GSM script. GSM scripts can be packaged into static TorchScript model and loaded into our GPUMD-GSM interface, offering out-of-the-box functionality for different enhanced sampling workflows.

After all CVs defined, they can be easily introduced into our predefined class template named MultiCVMetad, in which the internal computation and processing procedures of MetaD have already been implemented. Users only need to override the `_cal_bias` method to define their desired CV computations and combination processes within this method, returning both the bias and CV values. With this step, the GSM setup is all complete for MetaD simulations.

Once a GSM script is loaded into the GPUMD workflow, the GPUMD-GSM interface automatically extracts necessary data from the molecular dynamics process to perform enhanced sampling calculations. Numerical computations of CVs and corresponding bias-driven forces are computed in parallel using PyTorch tensor computation framework and automatic differentiation module. We designed input-output flows based on the GPUMD runtime processes to ensure the alignment of CV computation outputs with GPUMD outputs, named GPU-Sampling Trajectory Analysis (GSTA) module, facilitating post-processing and data analysis.

III. RESULTS AND DISCUSSION

A. Alanine dipeptide torsion

As one of the most classical benchmark systems in enhanced sampling simulations, alanine dipeptide was chosen as our test case [22–24]. In this fully GPU-accelerated workflow, we adopted Amberff19SB [25] as the ground truth according to previous studies [26], and sampled trajectories were subsequently used to construct a NeuroEvolution Potential (NEP) model [6,27]. The training details can be found in Fig.S2

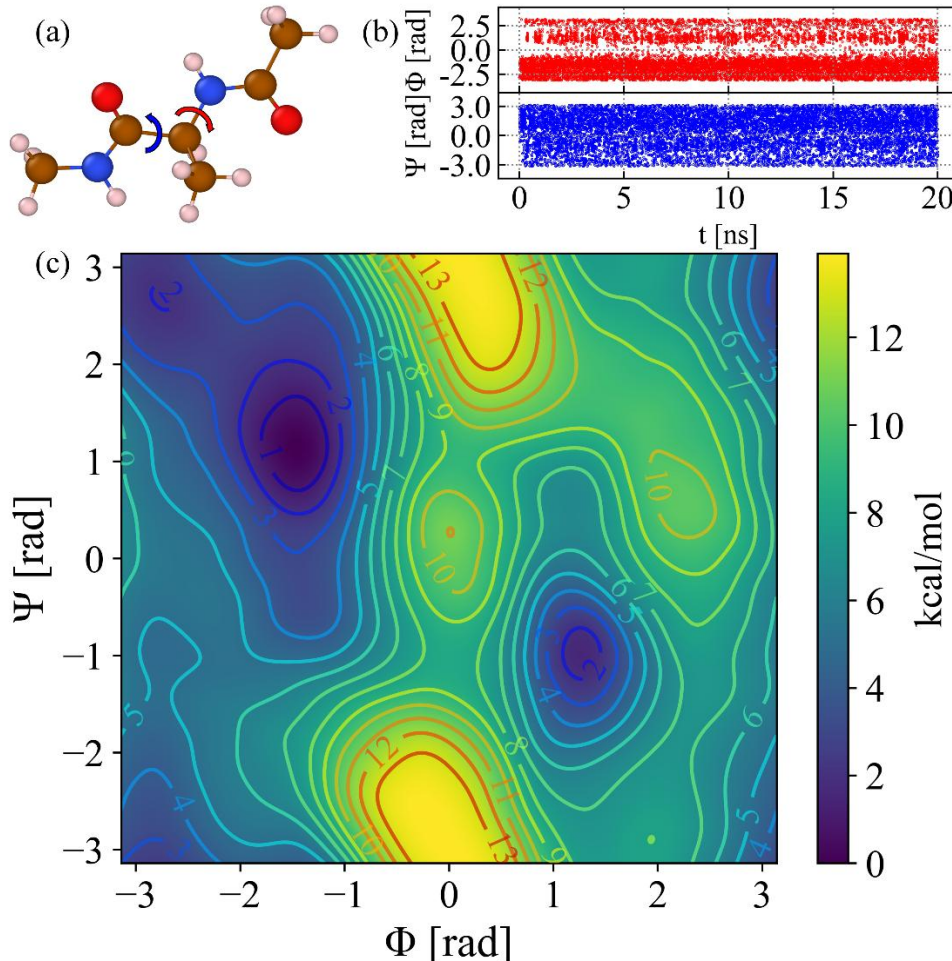


FIG 2. The 20ns NVT well-tempered metadynamics simulation result of alanine dipeptide. (a) The structure of alanine dipeptide. Red and blue arrows refer to torsion angles (Φ, Ψ) respectively. (b) The trajectory of CVs during the simulations. (c) Metadynamics rebuilt FES with two torsional angles.

In alanine dipeptide, the two backbone torsional angles annotated in Fig. 3b, $\Phi(\text{C-N-C}_\alpha\text{-C})$ and $\Psi(\text{N-C}_\alpha\text{-C-N})$, serve as the CVs as a typical scheme. We performed a 20 ns NVT well-tempered metadynamics simulation by setting $\sigma = 0.35$ rad, $W_k = 1.2$ kJ/mol, and the resulting FES is shown in Fig. 3a. Taking into account the intrinsic error of machine-learning force fields, our simulation successfully reproduced multiple metastable basins on the $\Phi-\Psi$ free energy landscape compared with previous works. Specifically, the simulation recovered the well-known minima corresponding to the right-handed α -helix region ($\Phi \approx -60^\circ$, $\Psi \approx -40^\circ$), the β -sheet region ($\Phi \approx -120^\circ$, $\Psi \approx 120^\circ$), as well as additional metastable states such as the left-handed α -helix region ($\Phi \approx 60^\circ$, $\Psi \approx 60^\circ$) [26].

B. water dissociation on rutile (110) surface

Water dissociation on the rutile (110) surface has long served as a prototypical system and has been extensively studied. In these typical oxide systems, surface oxygen atoms with dangling bonds can adsorb hydrogen atoms from water molecules, thereby promoting water dissociation. Consequently, determining the adsorption energy between surface oxygen atoms and hydrogen atoms from water is of great importance for understanding the mechanism of surface water splitting [16–18,28].

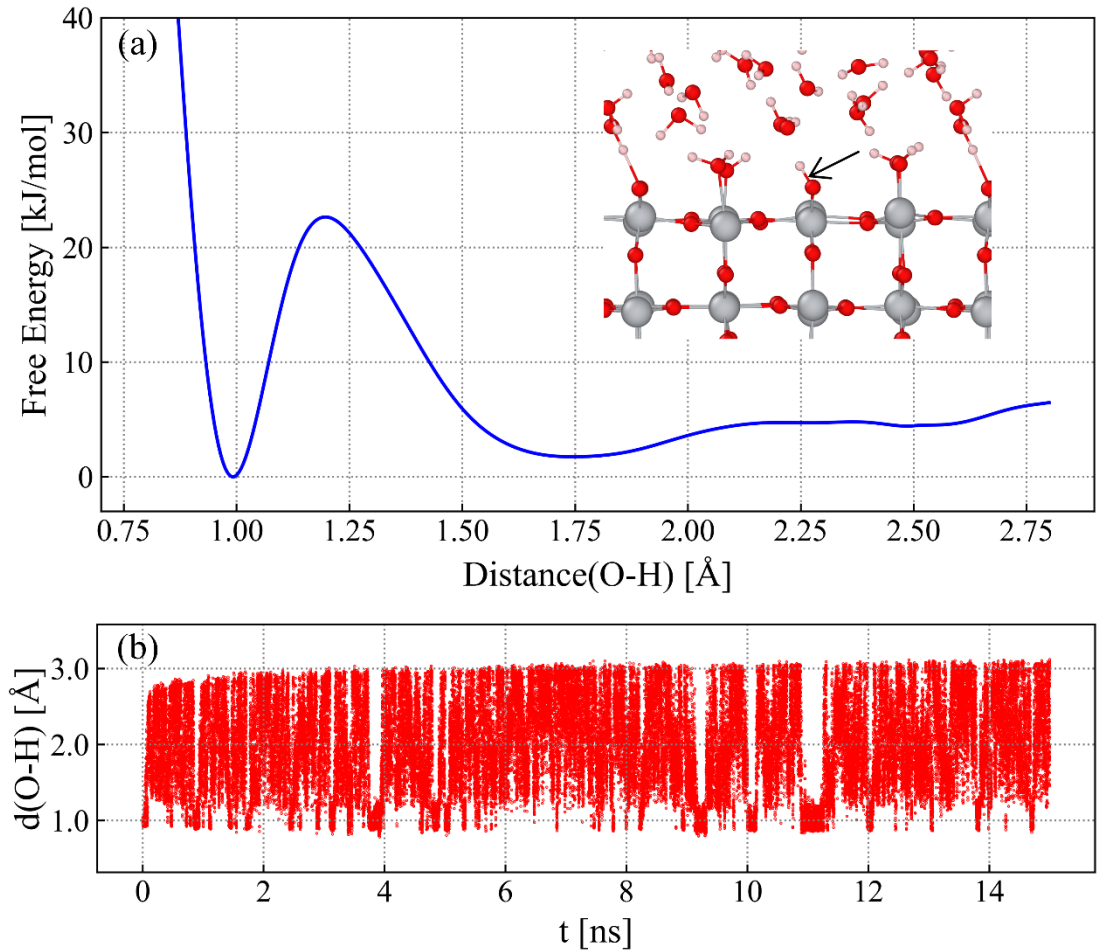


FIG 3. The NVT well-tempered metadynamics simulation result of water-rutile (110) interface. (a) The

FES of rutile (110) surface rebuilt by biasing on the bond of surface oxygen and hydrogen in water. The structure shows rutile (110) surface attached with water molecules where the black arrows points to the bond which we set as the CV. (b) The trajectory of CVs during the simulations.

From a publicly available dataset [18], we sampled 1918 rutile (110) surface configurations with adsorbed water molecules and trained a NEP model. The training details is illustrated in Fig.S3. Using the distance between a surface oxygen atom and its nearest hydrogen atom as the CV, we performed a 15 ns NVT well-tempered metadynamics simulation and reconstructed the corresponding free energy surface. Our calculations yield an adsorption energy barrier for the surface O–H bond of approximately 21.48kJ/mol, which agrees closely with previous reports within the uncertainty range of enhanced sampling methods. The simulation results highlight the consistency and convenience of our framework in achieving quasi-first-principles accuracy for surface catalytic processes.

C. B4-B1 phase transition in Large-scale systems

For solid-solid phase transitions, a classic example is the B4-B1 transition, which has been observed in numerous systems [29,30]. Gallium nitride, a prototypical semiconductor material, has been extensively studied. However, size effects remain a challenging issue for the B4-B1 phase transition [31,32]. Based on an open dataset [32], we trained a force field for GaN and performed metadynamics simulations for systems ranging from 27 thousand to 2.2 million atoms. In the larger-scale simulations, we successfully observed multi-site, plate-like nucleation during the phase transition.

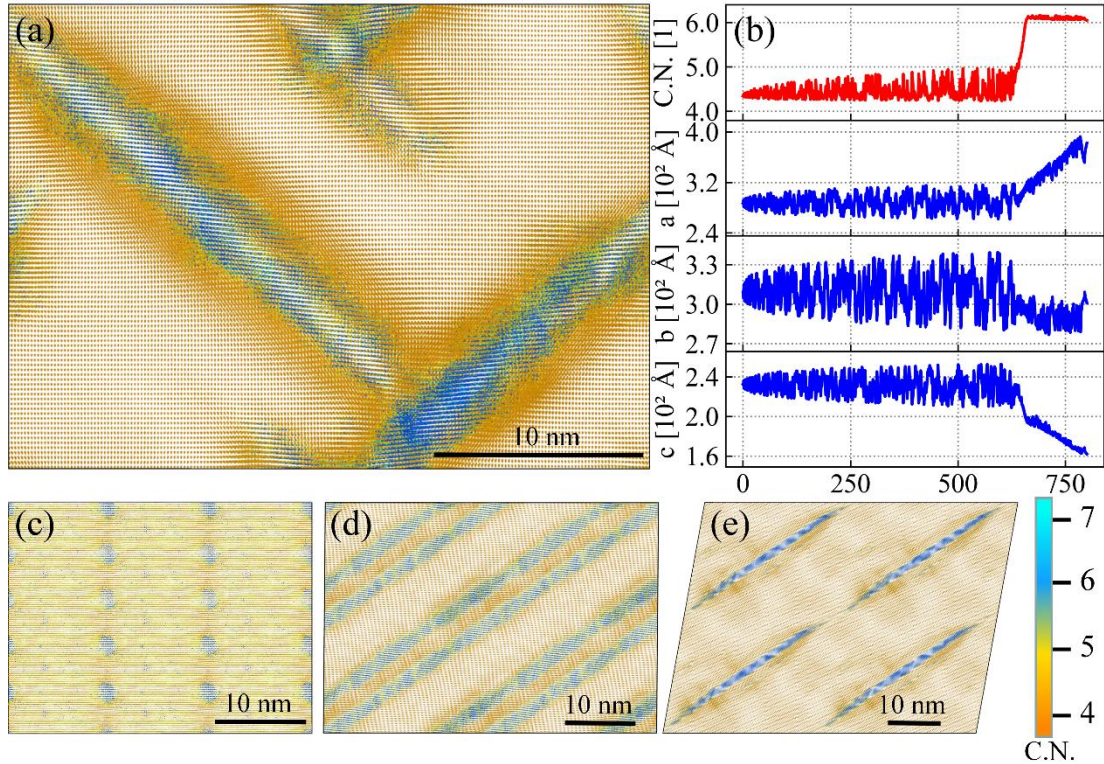


FIG 4. The metadynamics result of GaN B4-B1 phase transition in scales range from 27 thousand to 2.2 million atoms. (a) The structure with B1 nucleus in B4 phase colored by coordination numbers with 2.2 million atoms. (b) The CVs trajectory during simulation with 2.2 million atoms, indicating the multi-site, plate-like nucleation. We found a compression in c axis during the phase transition and a correspond expansion in a axis. (c-e) The structure of other different sizes, The systems have 3×5, 2×2, 2×2

replication for improved visualization, respectively. As the sizes enlarging, the simulations overcame the size effect and shows the plate-like nucleus.

We selected the coordination number (C.N.) and the triaxial lattice parameters as CVs. In simulation with 27648 atoms, we noticed that the lattice undergoes repeated compressive and tensile deformations, leading to a grid formed by bands of 5-coordinated atoms, in which the B1 phase with 6-fold coordination first nucleates. In simulations with 750,000 atoms or fewer, we observed the cooperative nucleation of a tilted strip-like B1 phase. Evidently, this strip touches the periodic boundary, indicating that the system still suffers from finite-size effects. In the 1.3 million atom simulation, we clearly identified a sheet-like B1 nucleus, which continued to grow toward the boundaries and eventually evolved into a strip, leading to the formation of the B1 phase. The simulation with 2.2 million atoms revealed a multi-site nucleation pathway, where numerous sheet-like B1 nuclei first appeared within the B4 phase. These nuclei gradually expanded and ultimately formed a polycrystalline B1 phase. Fig.5. presents the simulation results for systems containing 2.2 million atoms which provides clear evidence while other simulation details can be found in Supplementary Materials. By increasing the system size, we effectively mitigated finite-size effects and demonstrated the potential of our software package for uncovering novel physical mechanisms.

D. Efficiency of GSM package

We evaluated the hardware efficiency of this module in metadynamics simulations across different system sizes. Keeping the force field, dynamical parameters, and metadynamics parameters constant, we measured the simulation speed and hardware utilization on consumer-grade GPUs. Across simulations ranging from 50,000 to 1.3 million atoms, our GSM software package consistently demonstrates high computational efficiency, achieving performance comparable to that of pure GPUMD. In contrast, the more commonly used approach based on the LAMMPS[4] and Plumed[35] interface is approximately one order of magnitude slower than our method. The interface between GPUMD and Plumed suffers from performance bottlenecks due to GPU–CPU data transfer overhead and the lack of robust parallel support. As a result, not only is the computation significantly slower, but its performance further degrades as the system size increases. The detailed performance is shown in Figure 6. The test applied the same NEP model and our GSM framework ran on NVIDIA RTX4090, the lammps-plumed framework ran on Intel 9242 with 256G memory and the GPUMD-plumed framework, which needs both CPU and GPU computation ability, ran on a workstation with Intel 6230R*2 and NVIDIA RTX5880. Considering the loss of parallel efficiency from increasing the cores in CPU-based simulations, it can be asserted that our framework utilizes computational resources with maximum efficiency at a comparable cost, thereby enabling computations of larger systems.

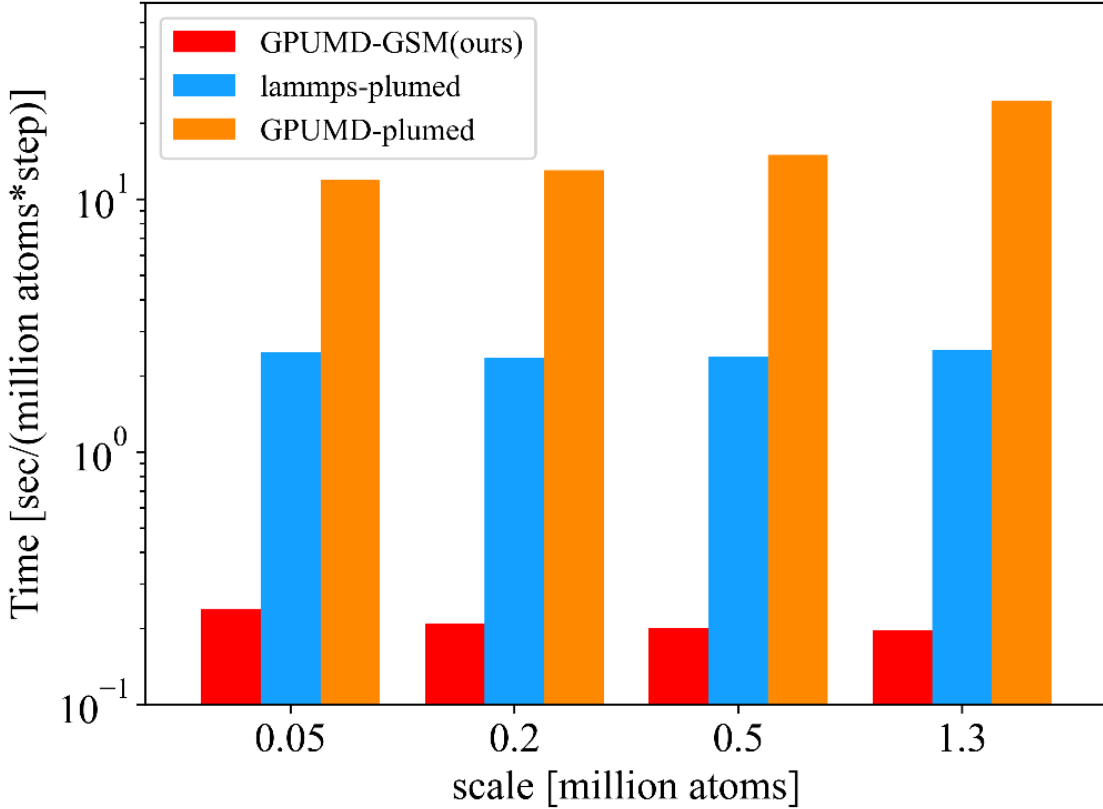


FIG 5. The real time cost of a one million atoms step simulation of different frameworks. The red bars represent our GSM packages which beats the mainstream lammps-plumed metadynamics frameworks with a speed advantages of over 10 times.

IV. CONCLUSIONS

In this work, we developed the GSM package to provide an intuitive, customizable, and user-friendly enhanced sampling scheme, which takes advantages in computational power and efficiency, especially for single-GPU computing. Moreover, our approach integrates with GPUMD and NEP, constituting a fully GPU-based metadynamics simulation solution. Users simply need to organize their datasets and select the CV to perform efficient metadynamics simulations with machine learning potentials on GPUs. In our future development plans, we aim to incorporate machine learning-based CV methods to make metadynamics simulations even more accurate and user-friendly. We envision that users will only need to organize a dataset or use a pretrained machine learning force field and supplement it with data relevant to the dynamic process under investigation to perform metadynamics simulations. We anticipate that GSM will pave the way for researchers seeking enhanced sampling simulations especially in large-scale systems, providing a powerful tool for investigating the dynamic mechanisms of crystals and polymer proteins.

ACKNOWLEDGMENTS

We gratefully acknowledge the financial support from the National Key R&D Program of China (grant no. 2022YFA1403201), the National Natural Science Foundation of China (grant number. T2495231, 12125404, 123B2049), the Basic Research Program of Jiangsu (Grant BK20233001, BK20241253), the

Jiangsu Funding Program for Excellent Postdoctoral Talent (2024ZB002, 2024ZB075), the Postdoctoral Fellowship Program of CPSF (Grant GZC20240695), the AI & AI for Science program of Nanjing University, and the Fundamental Research Funds for the Central Universities. The calculations were carried out using supercomputers at the High Performance Computing Center of Collaborative Innovation Center of Advanced Microstructures, the high-performance supercomputing center of Nanjing University.

REFERENCES

- [1] S. A. Hollingsworth and R. O. Dror, Molecular Dynamics Simulation for All, *Neuron* **99**, 1129 (2018).
- [2] M. Karplus and J. A. McCammon, Molecular dynamics simulations of biomolecules, *Nat. Struct. Biol.* **9**, 646 (2002).
- [3] G. M. Torrie and J. P. Valleau, Nonphysical sampling distributions in Monte Carlo free-energy estimation: Umbrella sampling, *J. Comput. Phys.* **23**, 187 (1977).
- [4] B. Roux, The calculation of the potential of mean force using computer simulations, *Comput. Phys. Commun.* **91**, 275 (1995).
- [5] I. Batatia, D. P. Kovacs, G. Simm, C. Ortner, and G. Csanyi, MACE: Higher Order Equivariant Message Passing Neural Networks for Fast and Accurate Force Fields, *Adv. Neural Inf. Process. Syst.* **35**, 11423 (2022).
- [6] K. Song et al., General-purpose machine-learned potential for 16 elemental metals and their alloys, *Nat. Commun.* **15**, 10208 (2024).
- [7] H. Wang, L. Zhang, J. Han, and W. E, DeePMD-kit: A deep learning package for many-body potential energy representation and molecular dynamics, *Comput. Phys. Commun.* **228**, 178 (2018).
- [8] J. Wang, Y. Wang, H. Zhang, Z. Yang, Z. Liang, J. Shi, H.-T. Wang, D. Xing, and J. Sun, E(n)-Equivariant cartesian tensor message passing interatomic potential, *Nat. Commun.* **15**, 7607 (2024).
- [9] T. Wang et al., Ab initio characterization of protein molecular dynamics with AI2BMD, *Nature* **635**, 1019 (2024).
- [10] D. E. Shaw et al., Atomic-Level Characterization of the Structural Dynamics of Proteins, *Science* (2010).
- [11] Y. Zhou, W. Zhang, E. Ma, and V. L. Deringer, Device-scale atomistic modelling of phase-change memory materials, *Nat. Electron.* **6**, 746 (2023).
- [12] R. Stocks, J. L. G. Vallejo, F. C. Y. Yu, C. Snowdon, E. Palethorpe, J. Kurzak, D. Bykov, and G. M. J. Barca, *Breaking the Million-Electron and 1 EFLOP/s Barriers: Biomolecular-Scale Ab Initio Molecular Dynamics Using MP2 Potentials*, in *SC24: International Conference for High Performance Computing, Networking, Storage and Analysis* (2024), pp. 1–12.
- [13] S. Angioletti-Uberti, M. Ceriotti, P. D. Lee, and M. W. Finnis, Solid-liquid interface free energy through metadynamics simulations, *Phys. Rev. B* **81**, 125416 (2010).
- [14] L. Bonati and M. Parrinello, Silicon Liquid Structure and Crystal Nucleation from Ab Initio Deep Metadynamics, *Phys. Rev. Lett.* **121**, 265701 (2018).
- [15] H. Niu, P. M. Piaggi, M. Invernizzi, and M. Parrinello, Molecular dynamics simulations of liquid silica crystallization, *Proc. Natl. Acad. Sci.* **115**, 5348 (2018).
- [16] J.-B. Le, A. Chen, L. Li, J.-F. Xiong, J. Lan, Y.-P. Liu, M. Iannuzzi, and J. Cheng, Modeling Electrified Pt(111)-Had/Water Interfaces from Ab Initio Molecular Dynamics, *JACS Au* **1**, 569 (2021).
- [17] B. Wen, M. F. Calegari Andrade, L.-M. Liu, and A. Selloni, Water dissociation at the water–rutile TiO₂(110) interface from ab initio-based deep neural network simulations, *Proc. Natl. Acad. Sci. U. S. A.*

120, e2212250120 (n.d.).

- [18] Z. Zeng, F. Wodaczek, K. Liu, F. Stein, J. Hutter, J. Chen, and B. Cheng, Mechanistic insight on water dissociation on pristine low-index TiO₂ surfaces from machine learning molecular dynamics simulations, *Nat. Commun.* **14**, 6131 (2023).
- [19] R. C. Bernardi, M. C. R. Melo, and K. Schulten, Enhanced sampling techniques in molecular dynamics simulations of biological systems, *Biochim. Biophys. Acta BBA - Gen. Subj.* **1850**, 872 (2015).
- [20] D. Quigley and P. M. Rodger, Metadynamics simulations of ice nucleation and growth, *J. Chem. Phys.* **128**, 154518 (2008).
- [21] B. Oruganti and R. Friedman, Activation of Abl1 Kinase Explored Using Well-Tempered Metadynamics Simulations on an Essential Dynamics Sampled Path, *J. Chem. Theory Comput.* **17**, 7260 (2021).
- [22] A. Barducci, G. Bussi, and M. Parrinello, Well-Tempered Metadynamics: A Smoothly Converging and Tunable Free-Energy Method, *Phys. Rev. Lett.* **100**, 020603 (2008).
- [23] M. Bonomi, A. Barducci, and M. Parrinello, Reconstructing the equilibrium Boltzmann distribution from well-tempered metadynamics, *J. Comput. Chem.* **30**, 1615 (2009).
- [24] D. Branduardi, G. Bussi, and M. Parrinello, Metadynamics with Adaptive Gaussians, *J. Chem. Theory Comput.* **8**, 2247 (2012).
- [25] C. Tian et al., ff19SB: Amino-Acid-Specific Protein Backbone Parameters Trained against Quantum Mechanics Energy Surfaces in Solution, *J. Chem. Theory Comput.* **16**, 528 (2020).
- [26] A. R. Tan, J. C. B. Dietschreit, and R. Gómez-Bombarelli, Enhanced sampling of robust molecular datasets with uncertainty-based collective variables, *J. Chem. Phys.* **162**, (2025).
- [27] Z. Fan et al., GPUMD: A package for constructing accurate machine-learned potentials and performing highly efficient atomistic simulations, *J. Chem. Phys.* **157**, (2022).
- [28] S. Meng, L. F. Xu, E. G. Wang, and S. Gao, Vibrational Recognition of Hydrogen-Bonded Water Networks on a Metal Surface, *Phys. Rev. Lett.* **89**, 176104 (2002).
- [29] B. Wu, Y. Li, Y. Lin, J. Liu, Y. Tao, X. Chang, and L. Lei, Determination of the B4-B1 phase boundary in semiconductors using isothermal compression Raman spectroscopy, *Appl. Phys. Lett.* **126**, 112109 (2025).
- [30] R. F. Zhang and S. Veprek, Deformation paths and atomistic mechanism of B4 → B1 phase transformation in aluminium nitride, *Acta Mater.* **57**, 2259 (2009).
- [31] P. A. Santos-Florez, H. Yanxon, B. Kang, Y. Yao, and Q. Zhu, Size-Dependent Nucleation in Crystal Phase Transition from Machine Learning Metadynamics, *Phys. Rev. Lett.* **129**, 185701 (2022).
- [32] Y. Yao and D. D. Klug, B 4 – B 1 phase transition of GaN under isotropic and uniaxial compression, *Phys. Rev. B* **88**, 014113 (2013).